Available online at www.sciencedirect.com
SCIENCE DIRECT®
Journal of Crystal Growth 254 (2003) 86–91
JOURNAL OF CRYSTAL GROWTH
www.elsevier.com/locate/jcrysgro

Effects of thermal treatment on the properties of ZnO films deposited on MgO-buffered Si substrates

S.J. Chen[a], Y.C. Liu[a,b,*], J.G. Ma[b], Y.M. Lu[b], J.Y. Zhang[b], D.Z. Shen[b], X.W. Fan[b]

[a] *Advanced Center for Optoelectronic Functional Material Research, Northeast Normal University, Changchun 130024, China*
[b] *Key Laboratory of Excited State Process, Changchun Institute of Optics, fine Mechanics and Physics, Chinese Academy of Sciences, 1-Yan An Road Changchun 130021, China*

Received 11 July 2002; accepted 6 March 2003
Communicated by R. James

Abstract

High quality ZnO thin films have been grown on Si (1 0 0) substrates with MgO buffer layers. An electron beam evaporation technique was used to grow MgO buffer layer on Si substrates followed by a magnetron sputtering process to deposit Zn films on the MgO-buffered Si substrates, next, a two-step annealing process was employed to oxidize the Zn films to form ZnO. The effects of the annealing temperature on the photoluminescence (PL) and orientation of ZnO nanocrystalline thin films were studied. For ZnO films annealed between 400°C and 700°C in an O_2 ambient, the quality of the ZnO films was improved with increasing annealing temperature. However, as the annealing temperature was increased to over 800°C, the ZnO film underwent a phase transformation from ZnO to a $Mg_xZn_{1-x}O$ alloy, where the x value in the alloy increased with increasing annealing temperature. The $Mg_xZn_{1-x}O$ alloy films were characterized by X-ray diffraction (XRD), photoluminescence (PL) and reflection spectra. XRD results show that the $Mg_xZn_{1-x}O$ alloy films maintain the hexagonal structure with a lattice constant close to that of ZnO. In films with Mg incorporation, intense ultraviolet band edge photoluminescence was observed at room temperature. The photoluminescence (PL) spectra show that $Mg_xZn_{1-x}O$ alloy has a wide band gap with a large exciton binding energy of 53 meV. The band gap of the $Mg_xZn_{1-x}O$ alloy shifts to higher energy with increasing annealing temperature. The blue-shift of the fundamental band gap of the alloy annealed at 1000°C is estimated to be ~300 meV.

PACS: 68.60.Dv; 78.55.Et; 81.15.Ef; 81.65.Mq

Keywords: A1. Crystal structure; A1. Photoluminescence; A1. X-ray diffraction; A3. Physical vapor deposition processes; B1. Zinc compounds; B2. Semiconducting II–VI materials

1. Introduction

ZnO has a direct band gap of 3.37 eV with a large exciton binding energy of 60 meV. Owing to the strong exciton binding energy, ZnO is

*Corresponding author. Key Laboratory of Excited State Process, Changchun Institute of Optics, fine Mechanics and Physics, Chinese Academy of Sciences, 1-Yan An Road Changchun 130021, China. Fax: +86-431-595-5378.
E-mail address: ycliu@nenu.edu.cn (Y.C. Liu).

0022-0248/03/$ - see front matter © 2003 Published by Elsevier Science B.V.
doi:10.1016/S0022-0248(03)01144-8

recognized as a promising photonic material in the UV region. Many different techniques, such as sputtering [1], reactive thermal evaporation [2], spray pyrolysis [3], pulsed laser deposition [4], metal organic chemical vapor deposition (MOCVD) [5], and molecular beam epitaxy (MBE) [6] have been used to prepare ZnO thin films. Magnesium oxide is thermodynamically very stable, has low dielectric constant and low refractive index, and has been widely used as a transition layer for growing various thin-film materials. The lattice of MgO crystals matches well with those of perovskite oxide crystals, as well as those of Si and GaAs crystals. MgO buffer layers were employed to grow high T_c superconductors [7,8] and ferroelectrics [9,10] as well as a nitride [11]. At the same time the ionic radius of Mg^{2+} is close to that of Zn^{2+} [12], so that the replacement of Zn by Mg is not expected to induce a significant change for the lattice constants of $Mg_xZn_{1-x}O$ alloys.

The growth and characterization of ZnO films on different substrates have been extensively studied [13–17], but little has been reported on the growth and characterization of ZnO films on Si with MgO buffer layers. In this paper, we reported results for ZnO films grown on Si substrates with MgO buffer layers. The ZnO films were deposited by RF planar magnetron sputtering of metallic Zn films, followed by a two-step anneal process in an oxygen ambient.

2. Experimental procedure

In the present study, an electron beam deposition system was used to prepare the MgO films, and a RF magnetron sputtering system was used to prepare the Zn films. MgO crystal and metallic zinc disks were used as the sputtering targets. Polished Si (1 0 0) wafers were used as the substrate. The Si substrates were cleaned using a standard Radio Corporation of America (RCA) cleaning procedure before deposition.

To deposit MgO films, the target-substrate spacing was kept at 25 cm, deposition pressure at 10^{-4} Pa, and substrate temperature at 400°C. The deposition was performed for 30 min. The thickness of the MgO films is about 600 nm. Next, about 500 nm of Zn film was deposited on the MgO film by RF magnetron sputtering.

After deposition, the films were oxidized in a thermal oxidation furnace. To prevent the evaporation of the metallic Zn from the films during the annealing process, we treated the films with a two-step annealing. All films were first oxidized in an oxygen ambient at 400°C for 2 h, then annealed in an oxygen ambient at 600°C, 700°C, 800°C, 900°C, 950°C, 1000°C, respectively. To characterize the crystal structure of these films, X-ray diffraction (XRD) was measured using a D/max-rA X-ray diffraction spectrometer (Rigaku) with a CuK_α line of 1.54 Å. Optical properties were characterized by photoluminescence (PL) and reflection spectroscopies. Photoluminescence (PL) spectra from 330 to 600 nm were measured at low temperature (from 77 to 300 K). The 325-nm line of a He–Cd laser with a power of 50 mW was used as the excitation light.

3. Results and discussion

The crystal structure and orientation of the films were investigated using $\theta - 2\theta$ scans of XRD. Results are shown in Fig. 1. A mixed pattern of ZnO and MgO peaks appears in the XRD spectra. Note that (1 0 0), (0 0 2) and (1 0 1) peaks of ZnO and (1 1 1), (2 0 0), and (2 2 0) peaks of MgO are

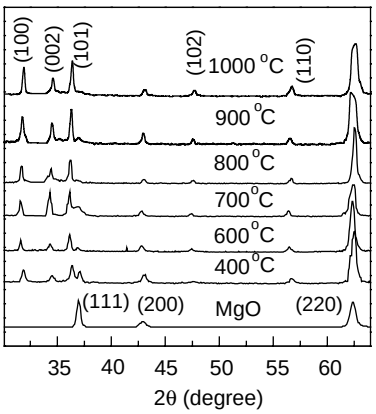

Fig. 1. XRD spectra of the annealed ZnO thin films and $Mg_xZn_{1-x}O$ alloy films with different annealing temperatures.

clearly seen. The XRD patterns indicate that the ZnO possesses a polycrystalline hexagonal wurtzite structure. The evaluated c-axis lattice constant of the ZnO film is 5.233 Å, which is quite close to the value of 5.207 Å obtained from a ZnO powder sample [18]. As the temperature increases from 400°C to 700°C, the (0 0 2) of ZnO peak becomes prominent in comparison to other peaks. Moreover, all the ZnO peaks become sharper with increasing annealing temperature due to increased particle size and improved crystal quality. It is seen that the peaks of the films shift to larger 2θ-angles with increasing annealing temperature from 800°C to 1000°C, leading to a decrease of the c-axis lattice constant. The results indicate that Mg^{2+} diffuses into the ZnO film and occupies the lattice site of Zn^{2+}. ZnO partially transforms to a $Mg_xZn_{1-x}O$ alloy partially, which causes the decrease of the c-axis lattice constant. The dependence of the c-axis lattice constant on annealing temperature is shown in Table 1. High annealing temperatures cause a decrease of the c-axis lattice constant due to the increase of Mg composition within the alloys.

Fig. 2 shows the room-temperature normalized PL spectra of ZnO films deposited on MgO-buffered Si (1 0 0) substrates annealed at different temperatures in the range of 400–1000°C. The main emission properties are closely dependent on the annealing temperature. The luminescence can be attributed to the strong near-band-edge (NBE) emission and the weak deep-level (DL) emission. As the annealing temperature increases from 400°C to 700°C, the NBE emission peak becomes sharper with a slight red-shift, and the DL emission peak intensity decreases. When the annealing temperature, however, increases to $T_a \geqslant 800$°C, the NBE emission intensity begins to decrease, the full-width at half-maximum (FWHM) increases, and the NBE emission peak position has an obvious blue-shift. When the annealing temperature increases up to 1000°C, the NBE emission peak positions has significantly shifted to a shorter wavelength, appearing at 3.57 eV with a narrower FWHM of 99 meV and very weak DL emission.

From the XRD patterns and PL spectra, it is confirmed that the ZnO film quality is gradually improved as the annealing temperature increases from 400°C to 700°C. At a sufficiently high annealing temperature, the strain from the distortion of the ZnO lattice is eliminated. The crystalline defects in the ZnO films decrease. As a result, the FWHMs of the PL spectra become more narrow with an increase in the annealing temperature, as shown in Fig. 3. When the annealing temperature, however, increases to $T_a \geqslant 800$°C, the FWHMs of the PL spectra begin to increase, and the NBE emission peak positions become distinctly blue-shifted. We believe that at higher annealing temperature Mg^{2+} and Zn^{2+} begin to diffuse mutually in the interface region, and ZnO undergoes a transformation from ZnO to an $Mg_xZn_{1-x}O$ alloy. This transformation would

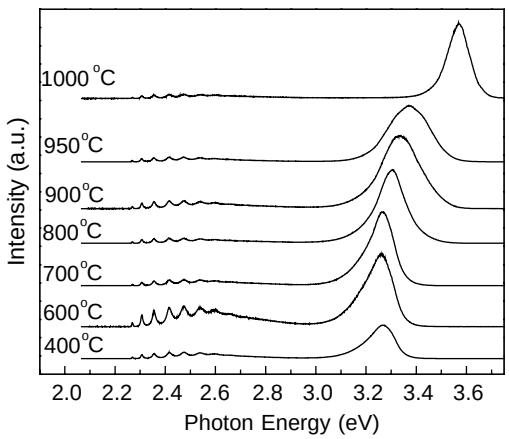

Fig. 2. Room temperature PL spectra of polycrystalline ZnO films and $Mg_xZn_{1-x}O$ alloy films annealed at different temperatures.

Table 1
The dependence of the c-axis lattice constant and Stokes-shift of the PL peak on the annealing temperature

Annealing temperature (°C)	400	600	700	800	900	1000
c-axis lattice constant (Å)	5.233	5.224	5.229	5.216	5.203	5.192
Stokes-shift of PL peak (meV)	159	123	89.7	109	162	186

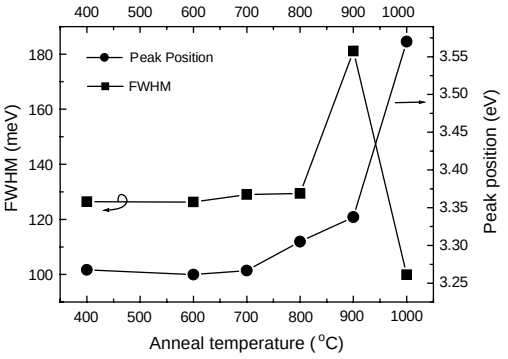

Fig. 3. The dependence of the FWHM and peak position of PL emission on annealing temperature.

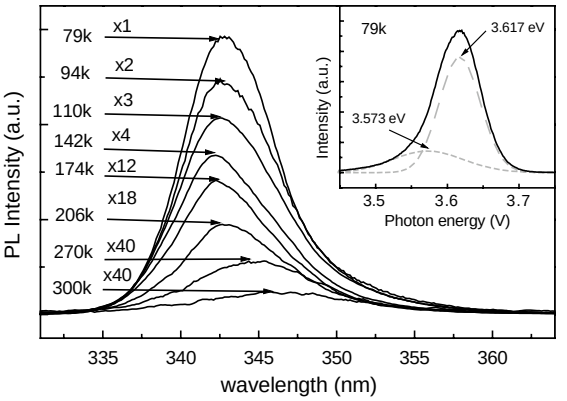

Fig. 4. PL spectra of the sample annealed at 1000°C measured at varied temperatures. Inset shows the results of the curve fitting calculation.

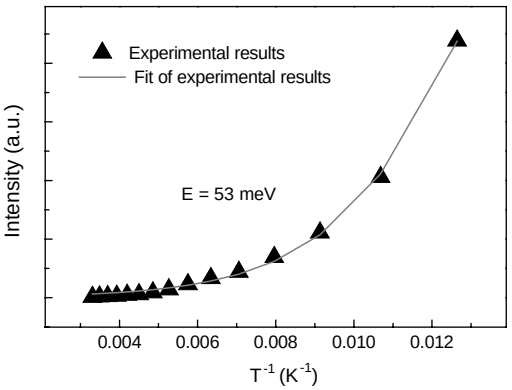

Fig. 5. The PL integrated intensity is plotted versus inverse temperature. Based on these data, the binding energy is estimated to be 53 meV.

broaden the band gap of the ZnO and make the crystal lattice more disordered. Higher annealing temperatures increase the Mg composition in the alloys. Thus, the NBE emission shifts to shorter wavelengths and the FWHMs of the PL spectra broaden with increasing annealing temperature. An increase in the FWHM values with increasing Mg content results presumably from fluctuations in the alloy composition, where localized excitons experience a different Coulomb potential. The exciton in $Mg_xZn_{1-x}O$ has a small Bohr radius, therefore, local (atomic scale) fluctuations of Mg content have an significant effect on the FWHM. As the annealing temperature increases up to 1000°C, a large number of Mg^{2+} enters into the Zn^{2+} lattice sites by diffusion. The ZnO totally transforms to a $Mg_xZn_{1-x}O$ alloy, and the lattice becomes ordered again at this high temperature. Thus, we observed a very strong emission peak at around 3.57 eV with a narrower FHWM of 99 meV and a very weak DL emission. This indicates that we can obtain high quality $Mg_xZn_{1-x}O$ alloy films with this method.

Fig. 4 shows the dependence of the PL spectra of the sample annealed at 1000°C on the sample temperature from 79 to 300 K. As the temperature increases, the NBE emission peak shifts to long wavelength side, and its intensity decreases remarkably. The results of the curve fitting calculation are also shown in the inset of Fig. 4. Two calculation curves perfectly fit our experimental results. The dominant peak is located at 3.57 eV, which is assigned to the bound exciton emission, i.e., the recombination of excitons trapped at shallow impurity levels. The weak feature is due to free exciton emission at around 3.62 eV. The Two emissions are much reduced and the free-exciton emission begins to be clearly visible with increasing temperature. At room temperature only the free-exciton emission remains. The quenching of the emission intensity with temperature was measured (see Fig. 5). To extract the binding energy, we fit the PL intensity to the equation [19,20] as follows:

$$I(T) = I_0\left[1 + C\exp(-E/kT)\right]^{-1}. \quad (1)$$

Here E is the binding energy of the exciton, and C contains ratios of optical-collection efficiencies

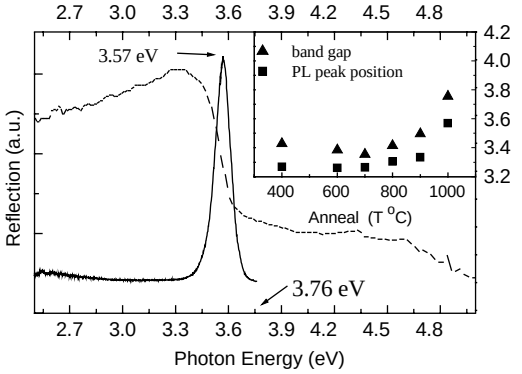

Fig. 6. Photoluminescence and reflection spectra taken at room temperature for the sample annealed at 1000°C. The inset shows the positions of the exciton absorption (measured by reflection) and emission peaks for all samples annealed at different temperatures.

and effective degeneracies of unbound and bound states. A careful fit to the data yields $E \approx 53$ meV for the sample annealed at 1000°C.

Fig. 6 shows the photoluminescence and reflection spectra taken at RT for the sample annealed at 1000°C. The positions of the exciton absorption (measured by reflection) and emission peaks for all samples annealed at different temperatures are plotted in the inset of Fig. 6. The luminescence peaks show a Stokes-shift toward the low-energy side of the absorption edge, as shown in Table 1. The broadening and Stokes shift of the luminescence peak are frequently observed in alloy semiconductors [21], where carriers feel different potentials depending on the local concentration and/or arrangement of the substituting elements. This effect is expected in ZnO, because the Bohr radius of excitons in ZnO is as small as 18 Å, so that excitons are more sensitive to local inhomogeneities.

4. Conclusions

In summary, ZnO thin films on Si (1 0 0) substrates with MgO buffer layers were obtained by two-step annealing of the metallic Zn film in an O_2 ambient. The quality of the ZnO films was improved with increasing annealing temperature from 400°C to 700°C. For annealing temperatures higher than 800°C, the ZnO underwent a transformation from ZnO to $Mg_xZn_{1-x}O$ alloy. When the annealing temperature increased up to 1000°C, the films totally transformed to a $Zn_xMg_{1-x}O$ alloy. The XRD studies of these films revealed hexagonal symmetry of the films for annealing temperatures between 400°C and 1000°C. The lattice constants of the films were close to that of ZnO. The Mg composition of the alloys increased with increasing alloying temperature from 800°C to 1000°C. The band gap of the hexagonal $Mg_xZn_{1-x}O$ films was determined to be approximately 3.76 eV.

Acknowledgements

This work was supported by the Program of CAS Hundred Talents, the National Natural Science Foundation of China, No.60176003, the Innovation Foundation of CIOFP, Excellent Young Teacher Foundation of Ministry of Education of China, and the Foundational Excellent Researcher to Go beyond Century of Ministry of Education of China.

References

[1] Sungale Cho, Jing Ma, Yunki Kim, Appl. Phys. Lett. 75. (1999) 2761.
[2] L.E. Brus, J. Chem. Phys. 80 (1984) 4403.
[3] H. Nanto, T. Minami, S. Takata, Phys. Stat. Sol. A 65 (1981) K131.
[4] H. Mprgan, D.E. Brodie, Can. J. Phys. 60.1387 (1982).
[5] J. Aronovich, A. Ortiz, R.H. Bube, J. Vac. Sci. Technol. 16 (1979) 994.
[6] R.D. Vispute, V. Talyansky, S. Choopun, R.P. Sharma, T. Venkatesan, M. He, X. Tang, J.B. Halpern, M.G. Spencer, Y.X. Li, L.G. Salamanca-Riba, A.A. Iliadis, K.A. Jones, Appl. Phys. Lett. 73 (1998) 348.
[7] F. Wang, S. Muller, R. Wordenweber, Thin Solid Films 232 (1993) 232.
[8] M.Z. Tseng, W.N. Jiang, E.L. Hu, J. Appl. Phys. 76 (1994) 3562.
[9] W.Y. Hsu, R. Raj, Appl. Phys. Lett. 60 (1992) 3105.
[10] D.K. Fork, G.B. Anderson, Appl. Phys Lett. 63 (1993) 1029.
[11] M. Tonouchi, Y. Sakaguchi, T. Kobayashi, J. Appl. Phys. 62 (1987) 961.

[12] A. Ohtomo, M. Kawasaki, T. Koida, K. Masubochi, H. Koinuma, Y. Sakurai, Y. Yoshida, T. Yasuda, Y. Segawa, Appl. Phys. Lett 72 (1998) 2466.
[13] B.T. Khuri-Yakub, G.S. Kino, P. Galle, J. Appl. Phys. 46 (1975) 3266.
[14] T. Shiosaki, S. Ohnishi, Y. Murakami, A. Kawabata, J. Crystal Growth 45 (1978) 346.
[15] T. Yamamoto, T. Shiosaki, A. Kawabata, J. Appl. Phys. 51 (1980) 3113.
[16] C.R. Aita, in: Proceedings of the IEEE Ultrasonics Symposium, 1980, p. 795.
[17] C.T. Lee, Y.K. Su, S.L. Chen, J. Crystal Growth 96 (1989) 785.
[18] Powder Diffraction File compiled by the Joint Committee on Powder Diffracrion, Card No. 36-1451.
[19] J.C. Kim, H. Rho, L.M. Smith, H.E. Jackson, S. Lee, M. Dobrowolska, J.K. Furdyna, Appl. Phys. Lett. 76 (1999) 214.
[20] R.E. Dietz, J.J. Hopfield, D.G. Thomas, J. Appl. Phys. 32 (1961) 2282.
[21] R. Zimmermann, J. Crystal Growth 101 (1990) 346.